

## Electronic Supplementary Information

### Symmetry Breaking Enhances the Catalytic and Electrocatalytic Performance of Core/Shell Tetrametallic Porous Nanoparticles

*Apoko S. Omondi, Dávid Kovács, György Z. Radnóczy, Zsolt E. Horváth, István Tolnai, András Deák, Dániel Zámbo\**

HUN-REN Centre for Energy Research, Budapest, Hungary

E-mail: [daniel.zambo@ek.hun-ren.hu](mailto:daniel.zambo@ek.hun-ren.hu)

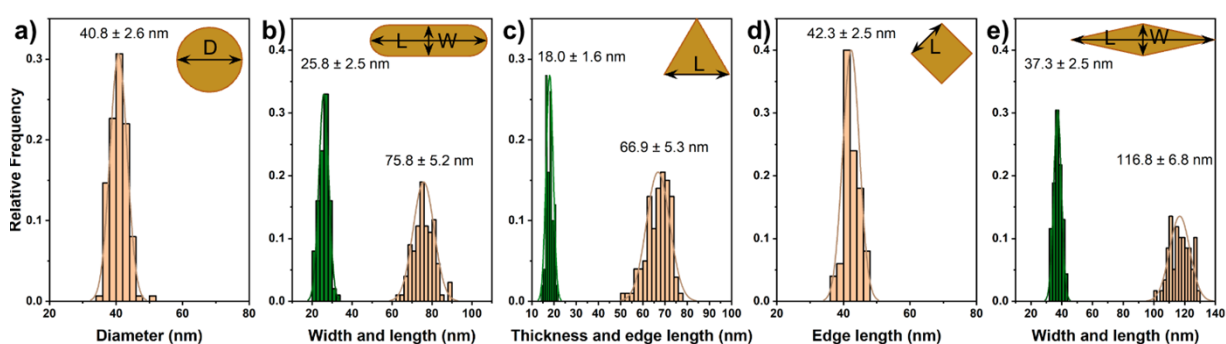


Figure S1. Size distribution of the synthesized Au core particles: nanospheres (a), nanorods (b), nanoprisms (c), nanooctahedra (d) and nanobipyramids (e). The measured characteristic dimensions are depicted in the schematics as insets of all panels.

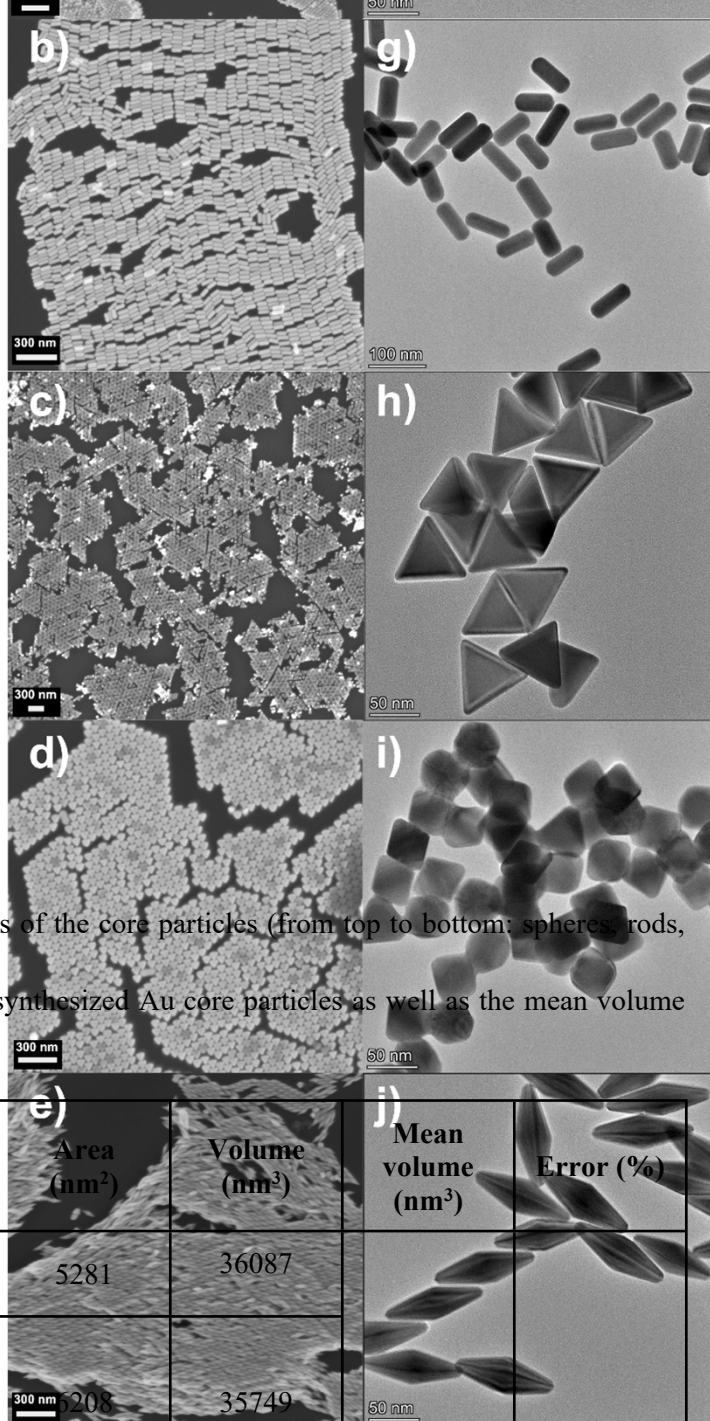


Figure S2. SEM (a-e) and TEM (f-j) images of the core particles (from top to bottom: spheres, rods, prism, octahedra and bipyramids)

Table S1. Dimensions and volumes of the synthesized Au core particles as well as the mean volume and its error for the five model systems.

NP type	Dimension	nm	Area (nm <sup>2</sup> )	Volume (nm <sup>3</sup> )	Mean volume (nm <sup>3</sup> )	Error (%)
AuNS	Diameter	41	5281	36087	35367	1.5
AuR	Length	76	208	35749		
	Width	26				
AuPrism	Edge length	67	7506	34988		
	Thickness	18				
AuOCT	Edge length	42	6111	34925		
AuBP	Length	117	7062	35087		
	Width	37				

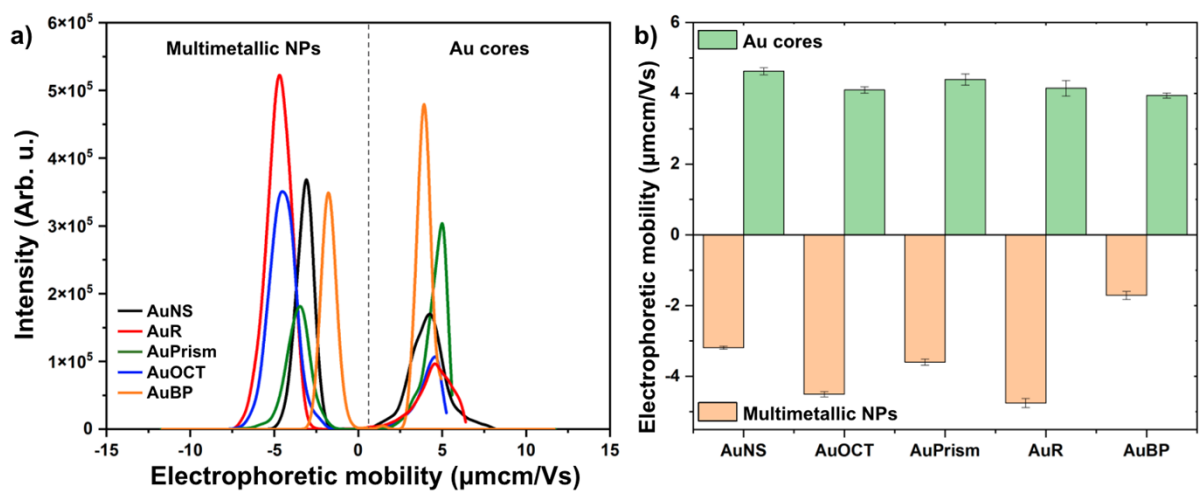


Figure S3. Electrophoretic mobility distributions (a) and the average mobilities (b) of the Au core and Au@mPdPtIr particles.

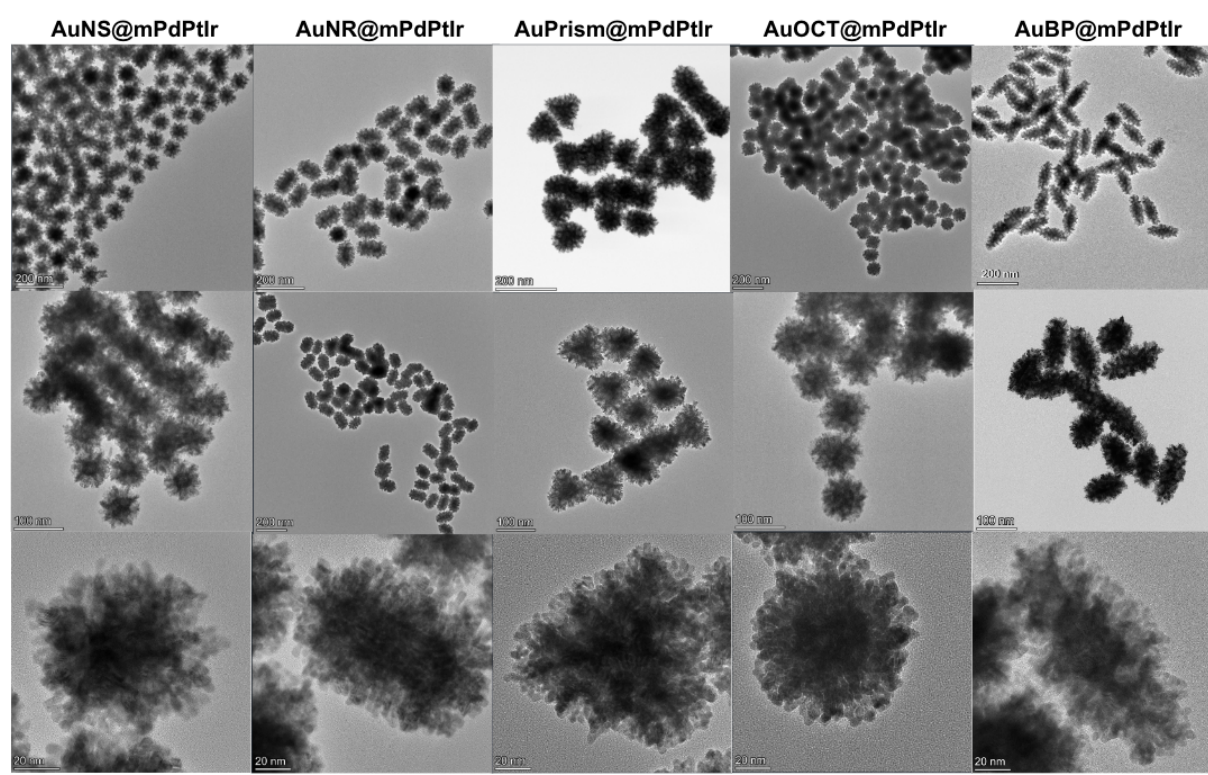


Figure S4. TEM images of the tetrametallic particles with spherical (a), rod-shaped (b), prism-shaped (c), octahedral (d) and bipyramidal (e) core in various magnifications.

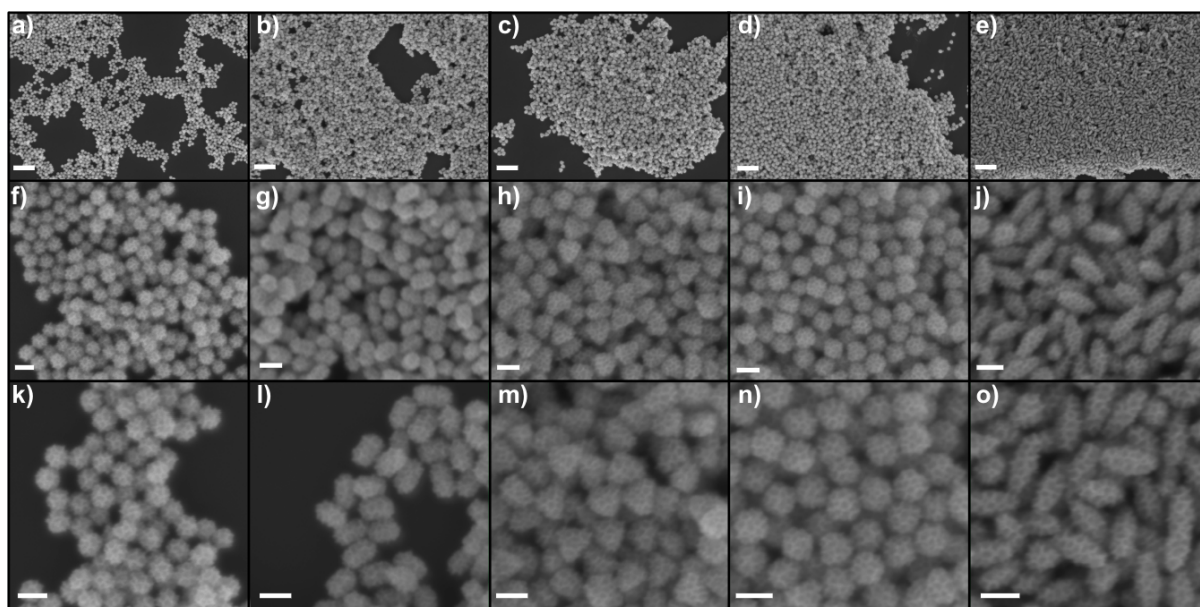


Figure S5. Representative SEM images in different magnifications of the tetrametallic Au@mPdPtIr particles with spherical (a,f,k), rod-shaped (b,g,l), prism-shaped (c,h,m), octahedral (d,i,n), and bipyramidal (e,j,o) core. Scale bars represent 500 nm, 100 nm and 100 nm for the first, second and third rows, respectively.

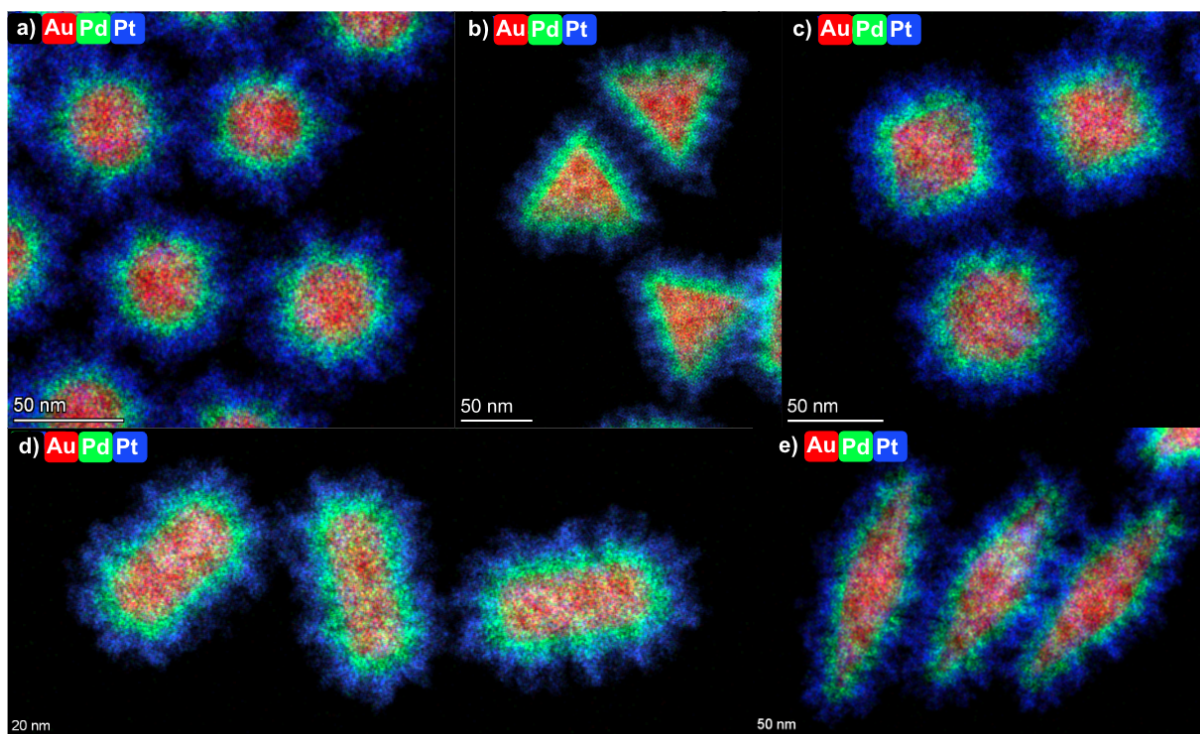


Figure S6. TEM-EDX elemental maps of the tetrametallic particles with spherical (a), prism-shaped (b), octahedral (c), rod-shaped (d), and bipyramidal (e) core. *Note: magnifications are different for a better visualization of the particles.*

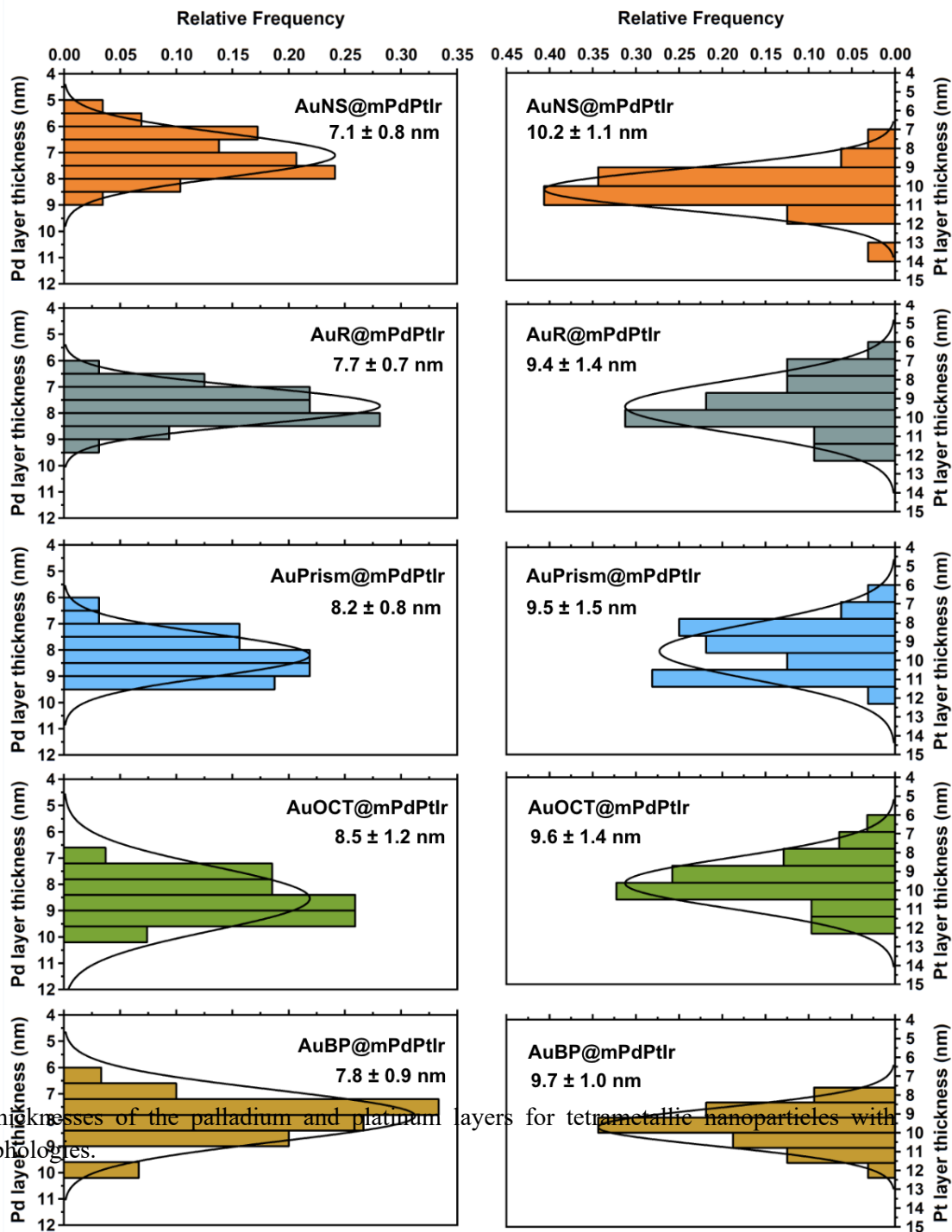


Figure S7. Thicknesses of the palladium and platinum layers for tetrametallic nanoparticles with different morphologies.

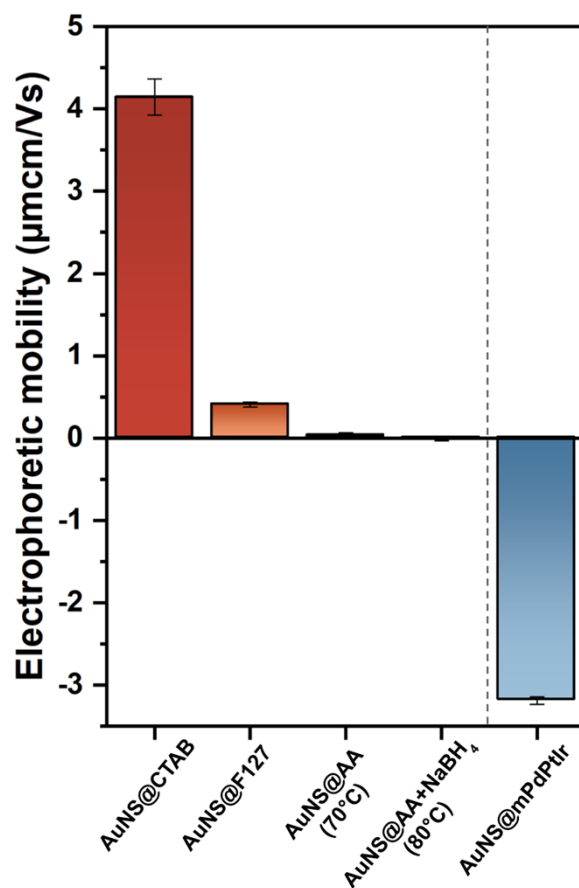


Figure S8. Electrophoretic mobilities of spherical Au core particles in a control experiment carried out in the same way as for the tetrametallic nanoparticles but using ultrapure water instead of the metal salts. The main steps of the synthesis: (i) AuNS in CTAB; (ii) washed with F127; (iii) addition of ascorbic acid at 70°C; (iv) addition of ascorbic acid and NaBH<sub>4</sub> solution at 80°C; (v) the final tetrametallic NPs for demonstrating the surface charge upon using metal salts.

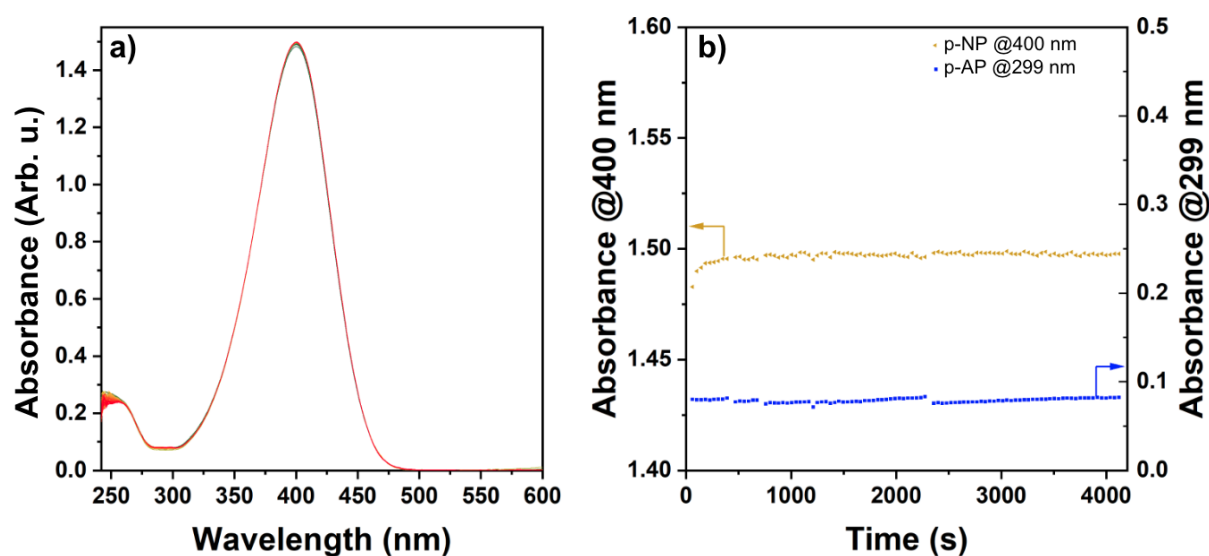


Figure S9. Time-resolved absorbance spectra of p-nitrophenol in the absence of the catalyst (a). Time is color coded by a green-to-red transition. Extracted absorbance values at 400 nm (for p-nitrophenol main peak) and 299 nm (for p-aminophenol) as a function of time (b).

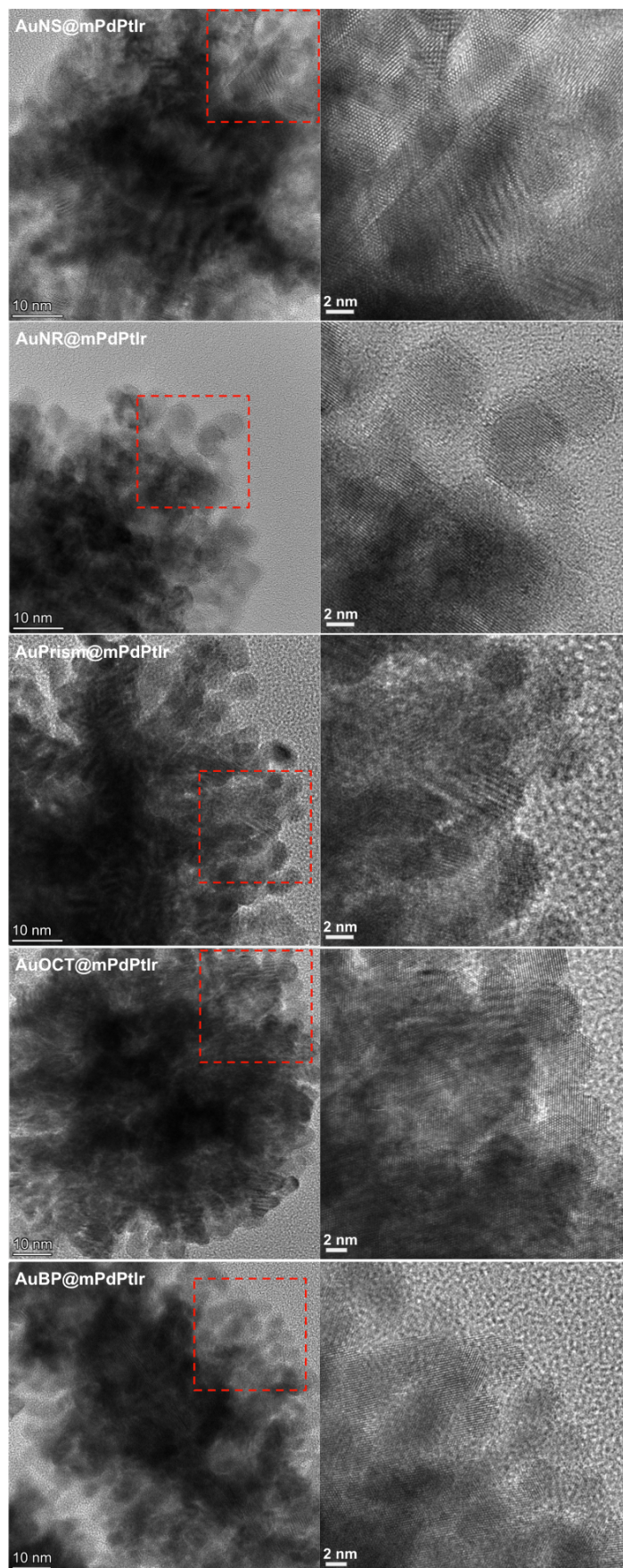


Figure S10. HR-TEM images of the tetrametallic NPs. Regions marked with red rectangles are enlarged in the right column.

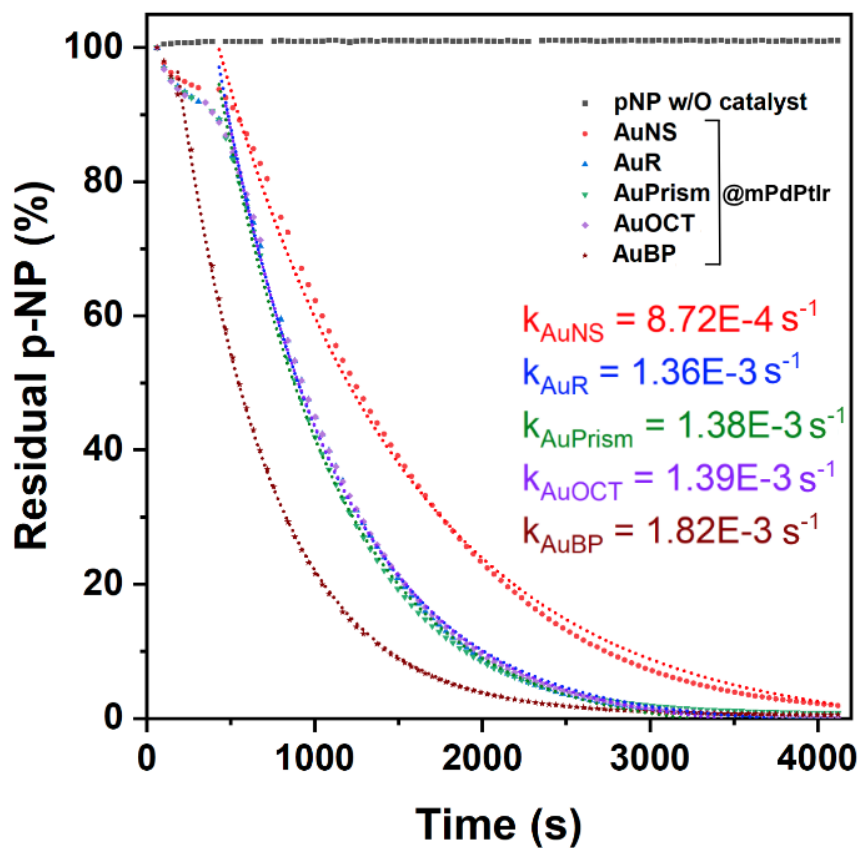


Figure S11. Pseudo-first order kinetics fitting of the residual pNP vs time data of the different multimetallic nanoparticles. Rate constants ( $k$ ) are listed with the corresponding color codes.

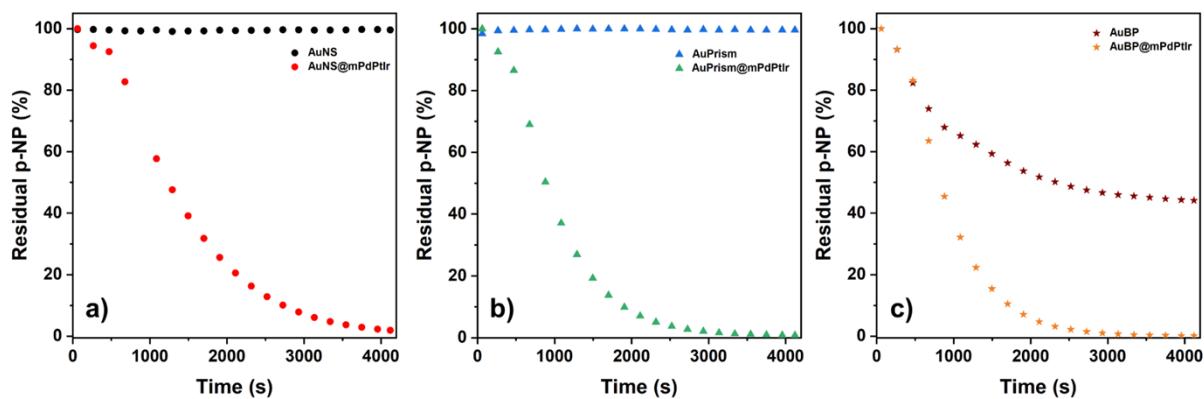


Figure S12. Time-dependent evolution of residual p-nitrophenol in control experiments using Au core particles instead of tetrametallic NPs: spheres (a), prisms (b) and bipyramids (c). All panels contain the dataset for the tetrametallic nanoparticles as reference.



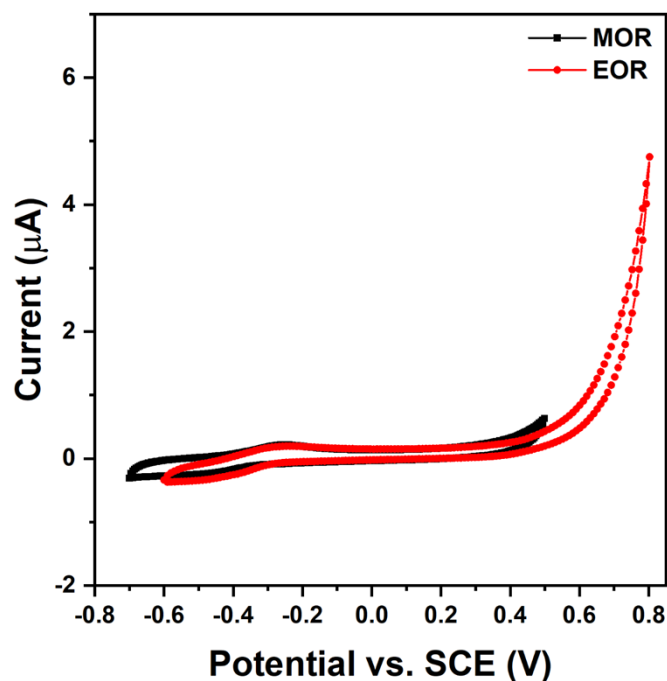


Figure S13. Voltammograms of glassy carbon electrodes in the absence of tetrametallic nanoparticles for MOR and EOR.

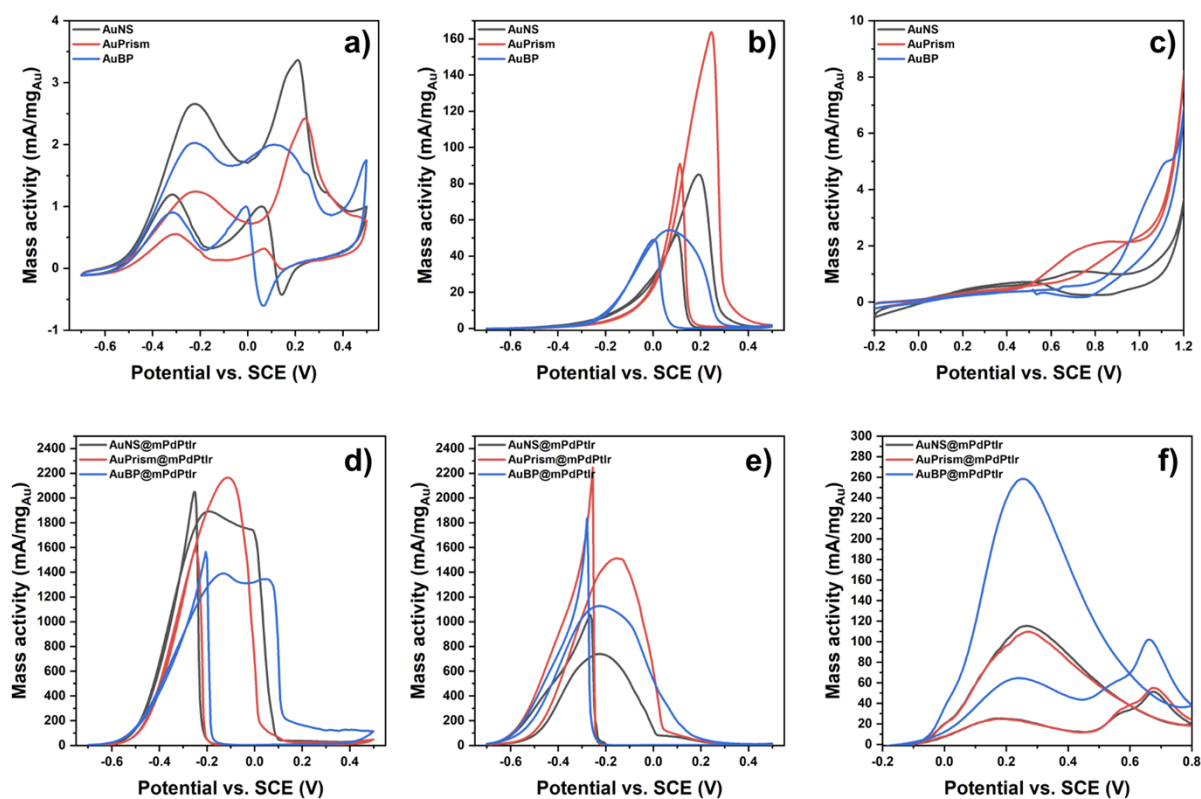


Figure S14. Mass activities for core only (a-c) and tetrametallic particles (d-f) in different electrocatalytic reactions: methanol oxidation reaction (a,d), ethanol oxidation reaction (b,e) and formic acid oxidation reaction (c,f). Mass activities are expressed in mA/mg<sub>Au</sub> units for a better comparison of the performances.